revised, Sept. 23, 2002

ON FACTOR GRAPHS AND ELECTRICAL NETWORKS

PASCAL O. VONTOBEL AND HANS-ANDREA LOELIGER*

Abstract. Factor graphs are graphical models with origins in coding theory. The sum-product and the max-product algorithms, which operate by message passing in a factor graph, subsume a great variety of algorithms in coding, signal processing, and artificial intelligence. In this paper, factor graphs are used to express a one-to-one correspondence (based on results by Dennis) between a class of static electrical circuits and multi-variable probability distributions; these factor graphs may also be viewed as variational representations of the electrical networks. For the classical linear state space models, both the sum-product algorithm and the max-product algorithm coincide with Kalman filtering. By the mentioned correspondence, these algorithms have a circuit theory interpretation that was discovered by Carter.

Key words. Factor graphs, Kalman filter, electrical networks, variational representations.

1. Introduction. Electrical engineers have always been using graphical models such as circuit diagrams, signal flow graphs, and many kinds of block diagrams. Other graphical models have developed in many other disciplines. Prominent among them are Markov random fields (e.g., [11]) with origins in statistical physics, and Bayesian networks [17] [13] [9] with origins in artificial intelligence.

The present paper is about factor graphs, a type of graphical model with origins in the theory of error correcting codes. Coding theory has been completely transformed during the last ten years as a consequence of the invention of turbo coding and the rediscovery of low-density parity-check codes [1]. With the recent refinements of these ideas, practical coding schemes are now available that virtually achieve the information theoretic capacity of many important communication channels. It is a common feature of all these new codes that they are naturally described by graphical models such as factor graphs. Moreover, all these codes are decoded by variations of a single algorithm, the sum(mary)-product algorithm, which operates by passing "messages" along the edges of the graph [1].

Graphs were implicit already in Gallager's work on low-density parity-check codes [8], and they were made explicit by Tanner [20]. What we now call a factor graph was essentially proposed by Wiberg et al. [24], [25] together with the sum-product and the max-product algorithms. Factor graphs were formally defined in [12]; it was recognized there that factor graphs subsume both Bayesian networks and Markov random fields and that the sum(mary)-product algorithm subsumes a wide variety of algorithms including Kalman filtering and the FFT. (For Kalman filtering, only

*Laboratory for Signal and Information Processing (ISI), Department of Information Technology and Electrical Engineering, ETH Zurich, Switzerland. The work of the first author was supported in part by ETH grant TH-16/99-3.

the scalar case was discussed in [12]; the vector/matrix case was worked out in [15]. An earlier graphical-model interpretation of Kalman filtering was given in [4] and [5]; see also [10].) Moreover, according to our growing experience, factor graphs are highly useful for the development of new algorithms, or new variations and combinations of known algorithms, in many detection and estimation problems.

In the present paper, however, we will say nothing about codes and very little about algorithms. Instead, we will use factor graphs to describe electrical networks. First, we will see how a static electrical network consisting of resistors, voltage sources, and current sources can be viewed as a factor graph. The basis for such an interpretation are results by Dennis [6], who showed that such electrical networks "solve" certain quadratic optimization problems. Second, we will see how some factor graphs can be translated into equivalent static electrical networks. This class of factor graphs includes the classical linear state space models of control theory, and the corresponding electrical networks are (discrete-time) Kalman filters and smoothers. We thus arrive at a circuit-theory interpretation of Kalman filtering that had been discovered by Carter [3].

The results of this paper do not appear to be practical, nor do we offer any really new mathematical theorem. Some insights have been gained, however:

- Electrical networks are an archetypical example of behavioral modelling in the sense of Willems [26]. Nevertheless, our factor graph of such a network can be interpreted as a nontrivial probabilistic model.
- Electrical networks operate not according to the sum-product algorithm, but according to the max-product algorithm. (For *linear* resistors, the two algorithms coincide.)
- Contrary to our expectation, Pontryagin duality (the Fourier transform) does not always work. For electrical networks, we have to use Lagrange duality.

Most known results on factor graphs and the sum(mary)-product algorithm require that the factor graph has no cycles. In the present paper, however, no such restriction applies anywhere.

We will, in fact, not use factor graphs as defined in [12], but a variation introduced by Forney [7] (there called "normal graphs"). The advantages of these Forney graphs were discussed in [7] and [15].

This paper is structured as follows. Section 2 is a self-contained introduction to Forney-style factor graphs. In Section 3, we discuss the elimination of "internal" variables, an important topic in system theory that is central to the factor graph formalism. In Section 4, we show how the results of [6] allow to view an electrical network as a factor graph. In Section 5, we discuss the duality between "voltage mode" and "current mode" factor graphs. In Section 6, we consider the translation of certain factor graphs into electrical networks; in particular, we show how the classical

linear state space models can be translated into electrical networks that "solve" the corresponding least squares or Kalman filtering (or smoothing) problem. It is then shown in Section 7 how the usual Kalman filtering and smoothing algorithms—i.e., the sum-product or max-product algorithm on Gaussian graphs—can be interpreted as manipulations of these electrical networks. Some conclusions are offered in Section 8. Some background material on normal distributions and on our use of the Dirac delta is given in the Appendix.

We will use the following notation. If f is a function $D \to \mathbb{R}$ with $D \subset \mathbb{R}$, we define

$$\int_x f(x) \triangleq \sum_{x \in D} f(x) \tag{1.1}$$

if D is a discrete set and

$$\int_x f(x) \triangleq \int_{-\infty}^{\infty} f(x)\, dx \tag{1.2}$$

if $D = \mathbb{R}$. More generally, for $D \subset \mathbb{R}^n$, we use this notation to integrate (or to sum) over the whole domain D of f. Of course, this notation can only be used in a context where this "definition" is not ambiguous.

The symbol $\propto$ will denote equality of functions up to a scale factor. This scale factor may be infinite: e.g., if $f : \mathbb{R}^2 \to \mathbb{R} : (x, y) \mapsto f(x, y)$ is continuous in x around $x = 0$, we will freely use expressions in the spirit of

$$\lim_{x \to 0} x f(x, y) \propto f(0, y) \tag{1.3}$$

and

$$\lim_{x \to 0} \frac{1}{x} f(x, y) \propto f(0, y). \tag{1.4}$$

2. Forney-Style Factor Graphs. Rather than the original factor graphs of [12], we will use *Forney-style factor graphs*. (These graphs were introduced in [7], where they were called "normal graphs".) A Forney-style factor graph (FFG) is a diagram as in Fig. 1 that represents the factorization of a function of several variables. E.g., assume that some function $f(x_1, \ldots, x_5)$ can be factored as

$$f(x_1, x_2, x_3, x_4, x_5) = f_{\mathrm{A}}(x_1, x_2, x_3) f_{\mathrm{B}}(x_3, x_4, x_5) f_{\mathrm{C}}(x_4). \tag{2.1}$$

This factorization is expressed by the FFG shown in Fig. 1. In general, an FFG consists of nodes, edges, and "half edges" (which are connected only to one node), and there are the following rules:

- There is a node for every factor.
- There is an edge (or half edge) for every variable.

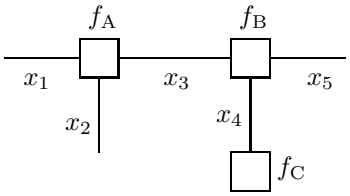

FIG. 1. *A Forney-style factor graph (FFG).*

- The node representing some factor g is connected with the edge (or half edge) representing some variable x if and only if x is an argument of g.

Implicit in these rules is the assumption that no variable appears in more than two factors; we will see below that this condition is far less restrictive than might appear at first sight.

The factors of the factorization expressed by the FFG are also called *local functions*; the overall function (i.e., the product of all local functions) is called the *global function*.

A *configuration* is a particular assignment of values to all variables. The *configuration space* Ω is the set of all configurations; it is the domain of the global function f. A configuration $\omega \in \Omega$ will be called *valid* if $f(\omega) \neq 0$.

In every fixed configuration, every variable has some definite value. We may therefore consider the variables in an FFG as functions of the configuration ω. It is often practical to mimic the standard notation for random variables and to denote such functions by capital letters. E.g., if x takes values in some set $\mathcal{X}$, we would write

$$X : \Omega \to \mathcal{X} : \omega \mapsto x = X(\omega). \tag{2.2}$$

A main application of factor graphs are probabilistic models. (In this case, the sample space can usually be identified with the configuration space Ω.) E.g., let X, Y, and Z be random variables that form a Markov chain. Then their joint probability mass function $p_{XYZ}(x, y, z)$ can be written as

$$p_{XYZ}(x, y, z) = p_X(x)\, p_{Y|X}(y|x)\, p_{Z|Y}(z|y). \tag{2.3}$$

This factorization is expressed by the graph of Fig. 2.

A block diagram (as in Fig. 3) may also be viewed as an FFG. Note that we have adopted the notation (2.2) for the variables. A function block $X_3 = g(X_1, X_2)$ in the block diagram is then interpreted as representing the factor

$$f_g(x_1, x_2, x_3) \triangleq \delta\big(x_3 - g(x_1, x_2)\big) \tag{2.4}$$

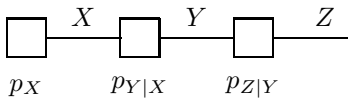

FIG. 2. *FFG of a Markov chain.*

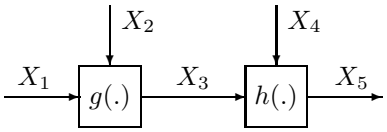

FIG. 3. *A block diagram.*

where $\delta(.)$ is the Kronecker delta function if X_3 is a discrete variable or the Dirac delta if X_3 is a continuous variable. The distinction between these two cases is usually obvious in concrete examples.

The block diagram of Fig. 3 expresses both the equations

$$X_3 = g(X_1, X_2) \tag{2.5}$$
$$X_5 = h(X_3, X_4), \tag{2.6}$$

and simultaneously and equivalenty the global function

$$f(x_1, \ldots, x_5) = \delta\big(x_3 - g(x_1, x_2)\big) \cdot \delta\big(x_5 - h(x_3, x_4)\big). \tag{2.7}$$

This function is nonzero if and only if the configuration is consistent with (2.5) and (2.6). Note that the arrows in the block diagram may help to define the factors, but are otherwise irrelevant for the interpretation as an FFG.

A block diagram usually contains also branching points as shown in Fig. 4 (left). In the corresponding FFG, such branching points become factor nodes on their own, as is illustrated in Fig. 4 (right). In doing so, there arise new variables (X' und X'' in Fig. 4) and a new factor

$$f_=(x, x', x'') \triangleq \delta(x - x')\delta(x - x''). \tag{2.8}$$

Note that $X = X' = X''$ holds for every valid configuration. By this device of variable "cloning", it is always possible to enforce the condition that a variable appears in at most two factors (local functions).

Nodes that represent frequently occuring local functions are often depicted using special symbols. We have just seen the symbol of Fig. 4 (right), which denotes an equality constraint as defined by (2.8). Another such symbol is shown in Fig. 5 and denotes a sum constraint. The leftmost part of Fig. 5 denotes the factor $\delta(x + y - z)$. Note that the arrows in Fig. 5

FIG. 4. *Branching point (left) becomes an equality constraint node (right).*

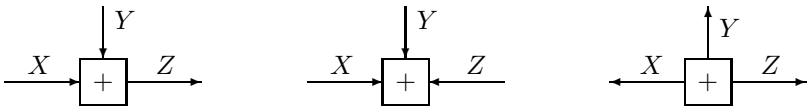

FIG. 5. *Sum constraint:* $X + Y = Z$ *(left) and* $X + Y + Z = 0$ *(middle and right).*

determine the sign of the variables. All combinations of directions of the arrows are well defined; e.g., both the middle and the right parts of Fig. 5 denote the factor $\delta(x + y + z) = \delta(-x - y - z)$.

The FFG in Fig. 6 with details as in Fig. 7 represents the classical equations of a linear state space model

$$X[k] = AX[k-1] + BU[k] \tag{2.9}$$

$$Y[k] = CX[k] + W[k], \tag{2.10}$$

with $k \in \mathbb{Z}$, where $U[k]$, $W[k]$, $X[k]$, and $Y[k]$ are real vectors and where A, B, and C are matrices of appropriate dimensions. In Kalman filtering, both $U[.]$ and $W[.]$ are usually assumed to be white Gaussian ("noise") processes; the corresponding nodes in these figures then represent factors $e^{-q(x)}$ for some quadratic form $q(x)$ (see the Appendix). The overall function whose factorization is expressed by Figs. 6 and 7 is the joint probability density of all involved variables.

If the variables $Y[k]$ are observed, say $Y[k] = y_k$, then these variables become constants; they may be absorbed into the involved factors and the corresponding branches may be removed from the graph. The graph then represents (the factorization of) the joint *a posteriori* density of all involved variables, up to a scale factor. We will come back to these figures in Section 6.

In most applications we are interested in the global function only up to a scale factor. (This applies, in particular, if the global function is a probability mass function.) We may then play freely with scale factors in the local functions. Indeed, the local functions are often defined only up to a scale factor. In this case, we would read Fig. 1 as expressing

$$f(x_1, \ldots, x_5) \propto f_{\mathrm{A}}(x_1, x_2, x_3) f_{\mathrm{B}}(x_3, x_4, x_5) f_{\mathrm{C}}(x_4) \tag{2.11}$$

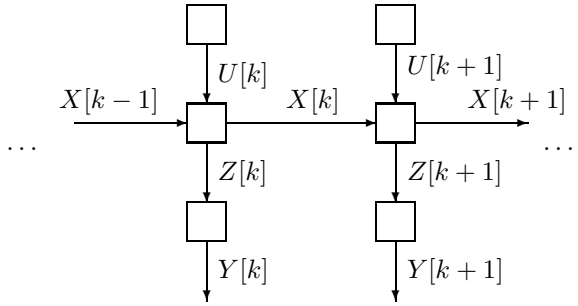

FIG. 6. *State space model.*

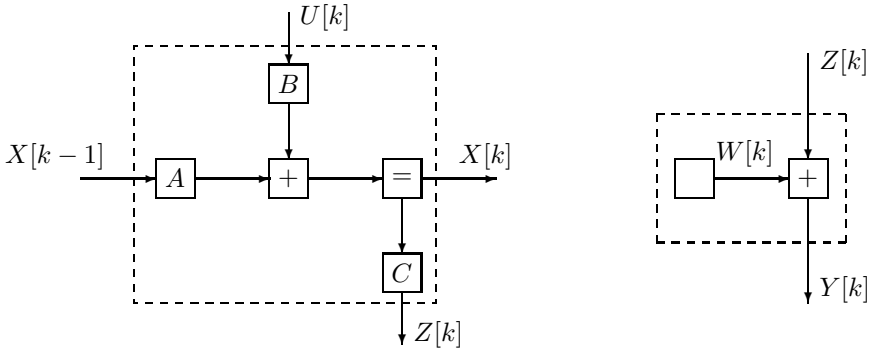

FIG. 7. *Details of linear state space model.*

instead of (2.1).

If all local functions are positive, it is natural to consider an FFG in the logarithmic domain. E.g., the factorization (2.1) may then be written as

$$-\log f(x_1, \ldots, x_5) = -\log f_{\mathrm{A}}(x_1, x_2, x_3) - \log f_{\mathrm{B}}(x_3, x_4, x_5) - \log f_{\mathrm{C}}(x_4). \tag{2.12}$$

In this way, the FFG may be viewed as an additive decomposition of the global function.

We will often find it permissible and convenient to view Dirac deltas as limits of normal distributions. (See the Appendix for details.) In this way, it will often be possible to satisfy the condition that all local functions are positive.

3. Composition of Systems and Elimination of Variables. As emphasized by Forney [7], the variables represented by half-edges should

be viewed as *external variables* and the variables represented by regular edges should be viewed as *internal variables*; the latter may also be called *hidden variables*, *latent variables*, or *state variables*.

The composition of two systems by indentification of variables corresponds to connecting some of the half edges of their FFGs. The connected edges are regular edges in the new FFG. Conversely, the decomposition of a system into subsystems may be expressed in the FFG by "drawing a box" around the internal variables of each subsystem, cf. Figs. 6, 7, and 8.

The operation of eliminating the internal variables of a subsystem ("closing the box") is of central interest in system theory. E.g., for a global function $f(x_1, \ldots, x_5)$, we might be interested in

$$f(x_1, x_2, x_3) = \int_{x_4} \int_{x_5} f(x_1, \ldots, x_5) \tag{3.1}$$

or in

$$f(x_1, x_2, x_3) = \max_{x_4} \max_{x_5} f(x_1, \ldots, x_5). \tag{3.2}$$

The general idea is to eliminate some of the variables by means of a "summary" operator, usually integration (or summation) or maximization (or minimization). Integration corresponds to marginalization in probability theory. Maximization, when applied to a $\{0, 1\}$-valued global function, may be viewed as the projection (to the remaining variables) of a set membership indicator function; "summarization" by maximization will also be crucial for the variational representation of electrical networks in Section 4. Note that only the valid configurations contribute to a sum or integral as in (3.1); if the global function is non-negative (e.g., a probability mass function), only the valid configurations contribute to a maximization as in (3.2).

For example, for the FFG in Fig. 8 (left), elimination of the internal variables by summation or integration yields

$$f(x) = \int_{x'} \int_{x''} g(x')h(x'')\delta(x - x')\delta(x - x'') \tag{3.3}$$

$$= g(x)h(x), \tag{3.4}$$

the product of g and h; for the FFG in Fig. 8 (right), we obtain

$$f(x) = \int_{x'} \int_{x''} g(x')h(x'')\delta(x - x' - x'') \tag{3.5}$$

$$= \int_{x'} g(x')h(x - x'), \tag{3.6}$$

the convolution of g and h.

FIG. 8. *Summarized function as product (left) and convolution (right) of two local functions.*

The elimination of variables by maximization raises a technical problem when Dirac deltas are involved. In the spirit of (1.4), we write

$$\max_x f(x,y)\,\delta(x-x_0) \propto f(x_0,y) \tag{3.7}$$

for any nonnegative function $f(x,y)$ that is continuous in x at x_0. Equation (3.7) defines the "summarized" function $f(x_0,y)$ only up to a scale factor, but as noted in Section 2, this suffices in most applications.

For the example in Fig. 8 (left), assuming that both g and h are nonnegative, we obtain

$$f(x) \propto \max_{x'} \max_{x''} g(x')h(x'')\delta(x-x')\delta(x-x'') \tag{3.8}$$

$$\propto g(x)h(x), \tag{3.9}$$

the same as (3.4) except for a scale factor; for the FFG in Fig. 8 (right), we obtain

$$f(x) \propto \max_{x'} \max_{x''} g(x')h(x'')\delta(x-x'-x'') \tag{3.10}$$

$$\propto \max_{x'} g(x')h(x-x'). \tag{3.11}$$

We will be particularly interested in the case where all local functions are of the form

$$f(x_1,\ldots,x_k) \propto e^{-q(x_1,\ldots,x_k)} \tag{3.12}$$

where $q(.)$ is a nonnegative definite quadratic form (see Appendix). In this case, the global function will also be of this form. In the logarithmic interpretation (cf. (2.12)), the FFG may then be viewed as an additive decomposition of a global quadratic cost function. Moreover, it follows from (A.5) and (A.6) that elimination of variables by integration coincides (up to a scale factor) with elimination of variables by maximization, which in turn obviously coincides with elimination of variables by minimization of the quadratic cost function.

For example, if both g and h in Fig. 8 (right) are normal distributions, then (3.11) can be written as

$$f(x) \propto \int_{x'} g(x')h(x-x'), \tag{3.13}$$

the same as (3.6) except for a scale factor.

FIG. 9. *A resistor (left) and a DC transfomer (right).*

4. Electrical Networks. We consider electrical networks as in Fig. 10 consisting of resistors, voltage sources, and current sources. In the example of Fig. 10, there are two resistors (R_1 and R_2), one voltage source (which forces the voltage accross the corresponding branch to be u_0), and one current source (which forces the current through that branch to be i_0). We use the letter U for voltages and the letter I for currents. The branches of such a network are directed, as indicated by the arrows in Fig. 10; these directions may be chosen at will. The usual description of such electrical networks uses two sets of variables: a current through each branch and a potential at each node. For a branch that starts at some node A and ends at some node B (see Fig. 9 left), we define the current through that branch as the current from A to B, and we define the voltage across that branch as the potential of A minus the potential of B.

These variables satisfy the following laws of physics:

Kirchhoff's current law: The sum of all currents at each node (with signs according to the arrows) is zero.

Kirchhoff's voltage law: The voltages can be derived from a potential (as defined above). Equivalently, the sum of all voltages along any cycle in the network is zero.

Branch laws: The voltage U and the current I for each branch are related as follows. For a resistor, we have $U = RI$ (Ohm's law) for some constant R. For a voltage source, we have $U = u_0$ for some constant u_0. For a current source, we have $I = i_0$ for some constant i_0.

We may allow also nonlinear resistors. The current I through, and the voltage U across, such a device (with the sign conventions of Fig. 9, left) satisfy $U = \rho(I)$, and we require ρ to be continuous and strictly monotonically increasing.

In Section 6, we will much use another circuit element, which (following Dennis [6]) we will call a *DC transformer*. The symbol for this element is shown in Fig. 9 (right), and its behavior is defined by the equations $U_2 = aU_1$ and $I_2 = -I_1/a$. If not specifically indicated, the parameter a equals one. In contrast to the other circuit elements, DC transformers do not appear to be easily realizable in practical circuits.

We now wish to interprete an electrical network as in Fig. 10 as an

FFG. If both voltages and currents are allowed to appear in the FFG, this is an easy task: just draw the FFG corresponding to the three laws (both Kirchhoff laws and the branch law for each branch). However, we are interested in an FFG that uses either currents or voltages, but not both.

Such FFGs do indeed exist. The voltages-only version is illustrated in Fig. 11. Each node of the electrical network is translated into an equality constraint. (Equality-constraint nodes of degree two may be omitted.) The arrows in the FFG are chosen exactly opposite to those in the electrical network. A resistor R between nodes A and B in the electrical network is translated into a factor

$$f_R(v_\mathrm{A}, v_\mathrm{B}, u) \triangleq \delta(v_\mathrm{A} - v_\mathrm{B} - u)e^{-\frac{u^2}{2R}} \tag{4.1}$$

where V_A and V_B denote the node potentials and where $U = V_\mathrm{A} - V_\mathrm{B}$ is the voltage accross the branch. Such a factor may also be written as

$$\int_u f_R(v_\mathrm{A}, v_\mathrm{B}, u) = e^{-\frac{(v_\mathrm{A}-v_\mathrm{B})^2}{2R}}. \tag{4.2}$$

Note that expressions such as (4.1) and (4.2) make sense only if we regard all quantities as dimensionless—or, equivalently, as normalized.

A voltage source is translated into a factor $\delta\left(v_\mathrm{A} - v_\mathrm{B} - u_0\right)$. A current source is translated into a factor $\delta(v_\mathrm{A} - v_\mathrm{B} - u)e^{-ui_0}$. A DC transformer as in Fig. 9 would result in a factor $\delta(u_2 - au_1)$. A nonlinear resistor would result in a factor

$$f_\rho(v_\mathrm{A}, v_\mathrm{B}, u) \triangleq \delta(v_\mathrm{A} - v_\mathrm{B} - u)e^{-\phi(u)} \tag{4.3}$$

with

$$\phi(u) \triangleq \int_0^u \rho^{-1}(s)\, ds. \tag{4.4}$$

If all resistors are linear and if we view the Dirac deltas as limits of normal distributions (see Appendix), the FFG thus obtained represents a normal distribution, up to a scale factor. (In some degenerate cases, the global function may not be integrable and is then not a probability distribution.) In the additive (i.e., logarithmic) interpretation, the FFG represents a quadratic function of all potentials.

THEOREM 4.1. *Assume that the electrical network has a unique solution (i.e., there is a unique assignment of currents and voltages that satisfies all three stated laws). Then these voltages achieve the unique maximum of the global function of the FFG.*

In the additive (logarithmic) interpretation of the FFG, the voltages achieve the unique minimum of the global quadratic function.

Proof. Consider the set of all configurations of voltages that

1. satisfy Kirchhoff's voltage law,

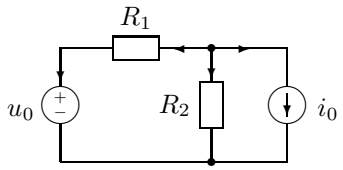

FIG. 10. *A simple electrical network.*

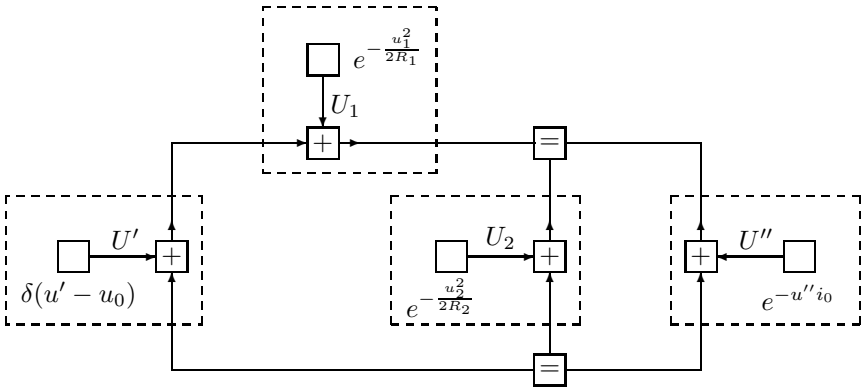

FIG. 11. *FFG (voltage version) corresponding to the electrical network of Fig. 10.*

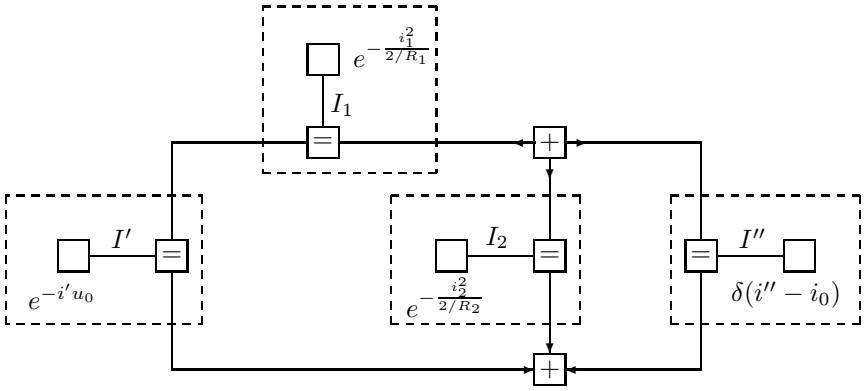

FIG. 12. *FFG (current version) corresponding to the electrical network of Fig. 10.*

2. comply with the specified voltage sources,
3. comply with the voltage ratios prescribed by the DC transformers.

Dennis [6, p. 35 ff.] proved that such a configuration of voltages gives rise (by means of the branch laws) to currents that satisfy Kirchhoff's current law if and only if the voltages minimize

$$\sum_k \frac{u_k^2}{2R_k} + \sum_\ell u_\ell i_\ell \tag{4.5}$$

where the first sum runs over all resistors and the second sum runs over all current sources (i.e., i_ℓ is prescribed). But (4.5) is exactly (the negative logarithm of) the global function represented by the FFG, apart from all the Dirac deltas that rule out the invalid configurations. □

Can we also have an FFG for such a circuit that uses currents instead of voltages?—The answer is "yes" and is illustrated in Fig. 12. We also have a theorem analogous to Theorem 4.1 above:

THEOREM 4.2. *Assume that the electrical network has a unique solution. Then these currents achieve the unique maximum of the global function of the (current-mode) FFG.*

Proof. Consider the set of all configurations of currents that

1. satisfy Kirchhoff's current law,
2. comply with the specified current sources,
3. comply with the current ratios prescribed by the DC transformers.

Dennis [6, p. 35 ff.] proved that such a configuration of currents gives rise (by means of the branch laws) to voltages that satisfy Kirchhoff's voltage law if and only if the currents minimize

$$\sum_k \frac{R_k i_k^2}{2} + \sum_\ell u_\ell i_\ell \tag{4.6}$$

where the first sum runs over all resistors and the second sum runs over all voltage sources (i.e., u_ℓ is prescribed). But (4.6) is exactly (the negative logarithm of) the global function represented by the FFG, apart from all the Dirac deltas that rule out the invalid configurations. □

Both theorems hold also for nonlinear resistors that satisfy the mentioned conditions. In this case, (4.5) should be changed into

$$\sum_k \phi_k(u_k) + \sum_\ell u_\ell i_\ell \tag{4.7}$$

(where the first sum still runs over all resistors, linear and nonlinear), and (4.6) should be changed into

$$\sum_k \tilde{\phi}_k(i_k) + \sum_\ell u_\ell i_\ell \tag{4.8}$$

with

$$\tilde{\phi}(i) \triangleq \int_0^i \rho(t)\, dt. \tag{4.9}$$

When we claim—as we do!—that an FFG as in Fig. 11 represents a system as in Fig. 10, we implicitly assume a summary operator (in the example: maximization). If all resistors are linear, we have seen that the global function (if it is integrable) may be viewed as a normal probability distribution. In this case, as we have seen in Section 3, maximization and integration are equivalent as summary operators.

It is tempting to speculate that an FFG as in Fig. 11 can be given a thermodynamic interpretation (cf. [3]), although no such thought was involved in its derivation.

5. Duality. Figs. 11 and 12 are obviously dual in some sense. However, other than in [7], the Fourier transform (Pontryagin duality) does not quite work here. What does work is a transformation of the global function based on Lagrange duality.

We describe this transformation by means of Fig. 13. We begin with the FFG in the top left of Fig. 13; its global function is

$$f(x_1, \ldots, x_5) = e^{-\phi_{\mathrm{A}}(x_1,x_2,x_3)} e^{-\phi_{\mathrm{B}}(x_3,x_4,x_5)} e^{-\phi_{\mathrm{C}}(x_4)}. \tag{5.1}$$

The variables $x_1, \ldots, x_5$ are real. The functions ϕ_{A}, ϕ_{B}, and ϕ_{C} are assumed to be real-valued, strictly convex (convex-$\cup$), and to have a continuous gradient. The global function (5.1) is transformed into

$$e^{-\phi^*_{\mathrm{A}}(y_1,y_2,y_3)} e^{-\phi^*_{\mathrm{B}}(y'_3,y_4,y_5)} e^{-\phi^*_{\mathrm{C}}(y'_4)} \delta(y_3 + y'_3) \delta(y_4 + y'_4) \tag{5.2}$$

where $\phi^*(.)$ denotes the conjugate function of $\phi(.)$, which we will discuss below. This transformation from (5.1) to (5.2) is illustrated in Fig. 13:

1. Top left to bottom left: each variable/edge in the original FFG is split into two variables/edges which are connected by an equality constraint.
2. Bottom left to bottom right: each factor $e^{-\phi(.)}$ is replaced by $e^{-\phi^*(.)}$, and all the auxiliary equality constraints are replaced by sum constraints.
3. Bottom right to top right: the new sum constraints may be absorbed as sign reversals into one of the adjacent factors.

It is obvious that this transformation of the FFG is analogous to the transformation corresponding to the Fourier transform [7].

We now come back to the conjugate function [2], [18], [6]. If $\phi : \mathbb{R}^n \to \mathbb{R}$ is convex with a continuous gradient, then its *conjugate function* (or *Legendre transform*) is the function $\phi^* : \mathbb{R}^n \to \mathbb{R}$ with

$$\phi^*(y) \triangleq \max_x \left(x^T y - \phi(x) \right). \tag{5.3}$$

The function $\phi^*(y)$ is also convex-$\cup$ and

$$\phi(x) = \max_y \left(x^T y - \phi^*(y)\right). \tag{5.4}$$

In the special case where

$$\begin{aligned} \phi(x) &= (x-m)^T W (x-m) + c & (5.5)\\ &= x^T W x - 2x^T W m + m^T W m + c, & (5.6) \end{aligned}$$

a quadratic form with a real positive definite matrix W, a straightforward calculation yields

$$\begin{aligned} \phi^*(y) &= \left(x^T y - \phi(x)\right)\big|_{x=\frac{1}{2}W^{-1}y+m} & (5.7)\\ &= \frac{1}{4} y^T W^{-1} y + m^T y - c. & (5.8) \end{aligned}$$

From (5.8), it is straightforward to give the transformation for each of the elements in Figs. 11 and 12. Linear resistors transform according to

$$e^{-\frac{x^2}{2R}} \longleftrightarrow e^{-\frac{y^2}{2/R}}. \tag{5.9}$$

Voltage sources and current sources transform according to

$$\delta(x-x_0) \propto \lim_{\beta\to\infty} e^{-\beta(x-x_0)^2} \longleftrightarrow \lim_{\beta\to\infty} e^{-\frac{y^2}{4\beta} - x_0 y} = e^{-y x_0}. \tag{5.10}$$

For any positive integer n, if V is any k-dimensional subspace of $\mathbb{R}^n$ with orthogonal complement $V^\perp$, we can use (A.12) to write

$$\delta(x \in V) \propto \lim_{\beta\to\infty} e^{-x^T W x} \tag{5.11}$$

for some positive definite matrix W that depends on β. It then follows from (A.15) that

$$\begin{aligned} \delta(y \in V^\perp) &\propto \lim_{\beta\to\infty} e^{-y^T W^{-1} y} & (5.12)\\ &\propto \lim_{\beta\to\infty} e^{-\frac{1}{4} y^T W^{-1} y}. & (5.13) \end{aligned}$$

It is thus clear from (5.8) that the negative logarithms of (5.11) and of (5.13) are conjugate functions, i.e.,

$$\delta(x \in V) \propto \lim_{\beta\to\infty} e^{-x^T W x} \longleftrightarrow \lim_{\beta\to\infty} e^{-\frac{1}{4} y^T W^{-1} y} \propto \delta(y \in V^\perp). \tag{5.14}$$

(This relation was already shown by Forney [7] for Pontryagin duality.) In particular, equality constraints and sum constraints transform into each

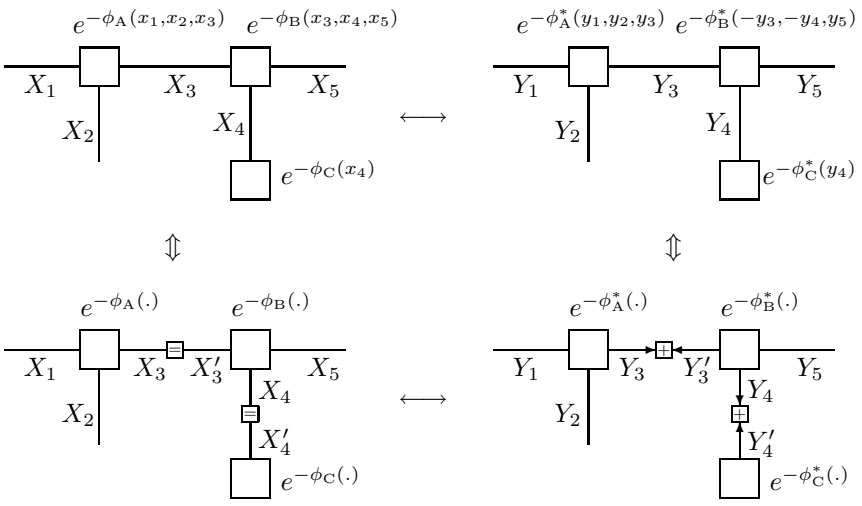

FIG. 13. *Dualization of an FFG (top left) using "mirror" variables.*

other: the set $V \triangleq \{(x_1, \ldots, x_n) \in \mathbb{R}^n : x_1 + \ldots + x_n = 0\}$ is an $n-1$-dimensional subspace of $\mathbb{R}^n$ and its orthogonal complement is the one-dimensional space $V^\perp = \{(y_1, \ldots, y_n) \in \mathbb{R}^n : y_1 = \ldots = y_n\}$. The duality of the DC transformer

$$\delta(x_2 - ax_1) \longleftrightarrow \delta(ay_2 + y_1) \tag{5.15}$$

follows also from (5.14) since $V \triangleq \{(x_1, x_2) \in \mathbb{R}^2 : -ax_1 + x_2 = 0\}$ and $V^\perp = \{(y_1, y_2) \in \mathbb{R}^2 : y_1 + ay_2 = 0\}$ are orthogonal complements of each other.

The transform of nonlinear resistors as in (4.3) is straightforward: by definition, we have

$$e^{-\phi(x)} \longleftrightarrow e^{-\phi^*(y)}. \tag{5.16}$$

In fact, it is not difficult to show that

$$e^{-\phi^*(y)} \propto e^{-\tilde{\phi}(y)}. \tag{5.17}$$

with $\tilde{\phi}$ as in (4.9).

6. From an FFG to an Electrical Network. We have seen how an electrical network can be interpreted as an FFG. We now consider the converse: the translation of an FFG into an electrical network. We consider FFGs consisting of the elements in Figs. 6 and 7: addition and equality

	voltage mode	FFG	current mode
1	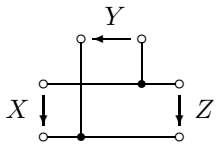	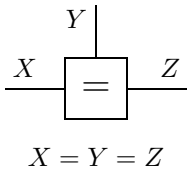	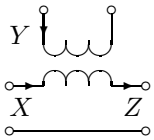
2	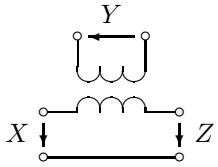	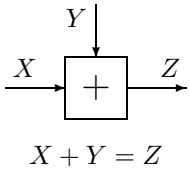	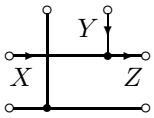
3	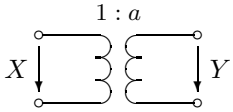	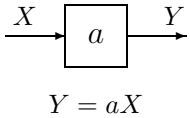	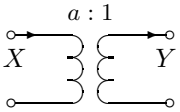
4	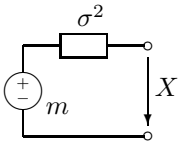	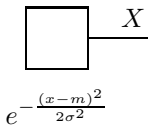	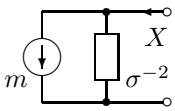

TABLE 1

Correspondence between the nodes in the FFG and the components of the electrical network.

of real vectors, the multiplication of such vectors by a real matrix, and normal probability distributions. More general probability distributions that correspond to nonlinear resistors (see (4.3)) can also be used.

We first consider the case where all variables are scalars. The translation from the FFG to an electrical network is given in Table 1. Each variable is represented by two wires. There are two versions, which are dual to each other. In the voltage version, a variable is represented as the voltage between the two wires. In the current version, a variable is represented as the current through one of the wires. (The current through the

other wire will be the same, but in the opposite direction).

A circuit constructed according to Table 1 can often be simplified by the elimination of transformers as shown in Fig. 14. For example, if either of the FFGs of Figs. 11 or 12 is translated into a circuit according to Table 1, all transformers can be eliminated and the original circuit of Fig. 10 results.

A vector variable $X = (X_1, \ldots, X_n)^T$ with real $X_1, \ldots, X_n$ is represented by $n + 1$ wires. The extra wire is the reference potential for all voltages. The circuits for vector addition are given in Fig. 15. These two circuits operate also as vector-equality constraints: the current-mode adder (Fig. 15 (right)) is also a voltage-mode equality constraint and the voltage-mode adder (Fig. 15 (left)) is a current-mode equality constraint.

Fig. 16 shows a voltage-mode circuit for the multiplication

$$\begin{pmatrix} Y_1 \\ Y_2 \end{pmatrix} = \begin{pmatrix} a & b \\ c & d \end{pmatrix} \cdot \begin{pmatrix} X_1 \\ X_2 \end{pmatrix}. \tag{6.1}$$

In the reverse direction, this same circuit works as a matrix-times-vector multiplier in current mode. The generalization of this circuit to arbitrary $n \times n$ matrices is obvious.

An FFG from these elements will usually describe a global function with a unique global maximum. (It is easy to construct an FFG that has no valid configuration, but such cases are usually easily excluded.) In this case, as we have seen in Section 4, the electrical network will settle in the (unique) global maximum of the global function. For example, if the FFG represents a Kalman filtering (or smoothing) problem, then the electrical network will settle in the desired Bayesian (or least squares) solution.

7. Circuit-Theory Interpretation of Message Passing. It is well known that (discrete-time) Kalman filtering and smoothing may be viewed as "message passing" algorithms in a graphical model [4] [5] [10] [14]. In particular, it was pointed out in [12], and worked out in more detail in [15], that Kalman filtering and smoothing are instances of the sum-product algorithm, which operates by passing messages along the edges of the factor graph. The messages consist of mean vectors and covariance matrices (or inverses of covariance matrices) that are computed according to the rules of the sum-product algorithm. In its most narrow sense, Kalman filtering is only the forward sum-product recursion through the graph of Fig. 6 and yields the a posteriori probability distribution of the state $X[k]$ given the observation sequence $Y[.]$ up to time k. By computing also the backward messages, the a posteriori probability of all quantities given the whole observation sequence $Y[.]$ may be obtained. More generally, Kalman filtering amounts to the sum-product algorithm on any FFG (or part of an FFG) that consists of (the vector/matrix versions of) the linear building blocks listed in Table 1 (middle column).

As shown in Section 6, the Kalman filtering *problem* may be translated into a static electrical network. The Kalman filtering and smoothing

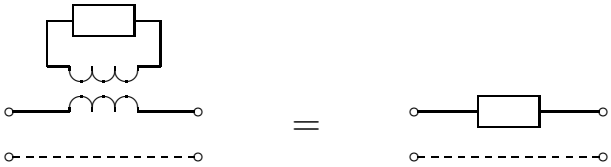

FIG. 14. *Elimination of a transformer.*

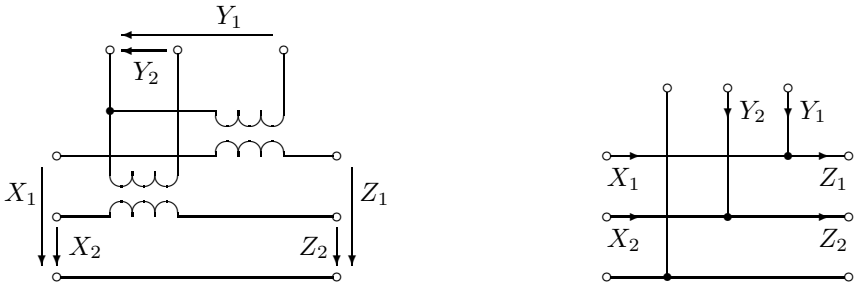

FIG. 15. *Vector addition $Z = X + Y$: voltages (left) and currents (right).*

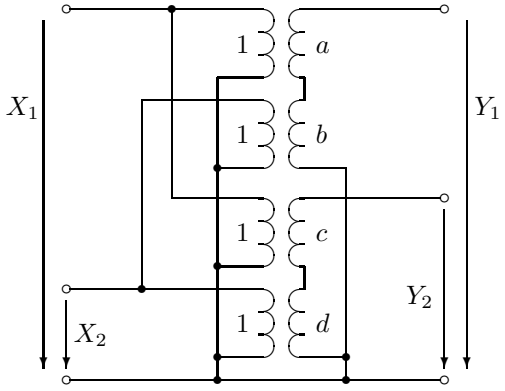

FIG. 16. *Matrix multiplication (voltage mode).*

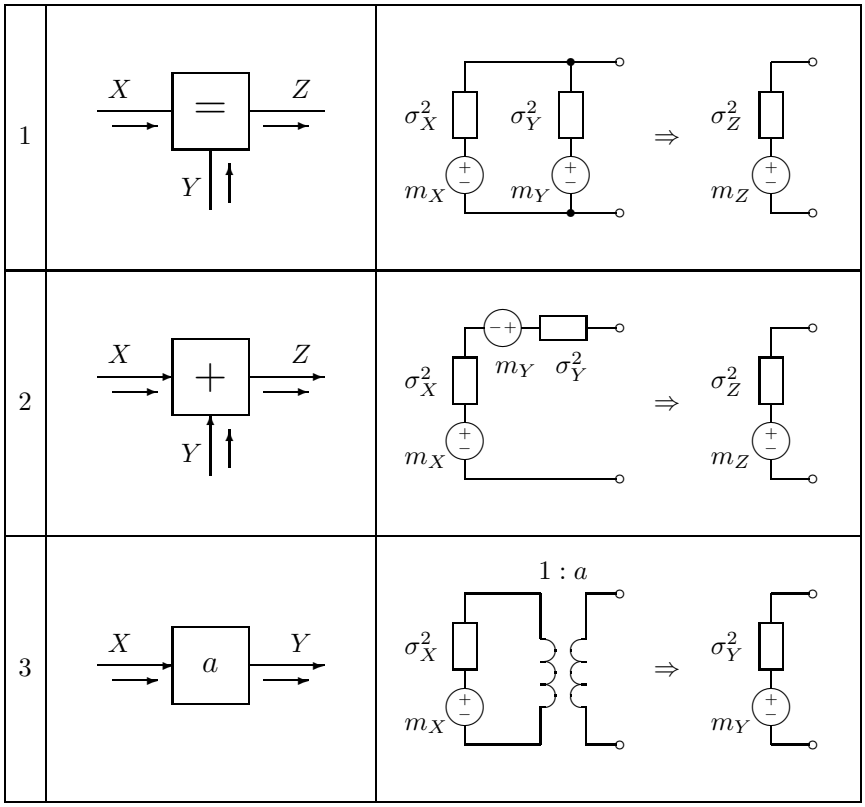

TABLE 2
Circuit interpretation of message computation.

algorithm (i.e., sum-product message passing through the FFG) may then be interpreted as manipulations of the electrical network. Each message represents a Gaussian distribution and may thus be represented by a corresponding electrical network, as shown (for the scalar case) in the bottom row of Table 1. As illustrated in Table 2, the computation of messages out of the other node types in Table 1 then amounts to connecting the incoming messages/circuits to the node circuit and reducing the resulting circuit to its Thévenin equivalent circuit (i.e., a voltage source in series with a resistor) or its Norton equivalent circuit. This interpretation of Kalman filtering was discovered by Carter [3].

As is obvious from Theorems 4.1 and 4.2, electrical networks "run" by the max-product algorithm rather than by the sum-product algorithm. If all resistors are linear, the corresponding FFG is a Gaussian network, in which case the max-product algorithm coincides with the sum-product

algorithm (cf. [15]).

If the max-product message passing algorithm converges, then the unique maximum of the global function is reached [23] and [19]. However, the message passing algorithm may fail to converge, while the electrical network will always settle in the maximum of the global function.

8. Conclusions. We have seen that any static electrical network consisting of linear (or monotonically nonlinear) resistors, voltage sources, and current sources can be viewed as a Forney-style factor graph (FFG) in either currents or voltages alone. This representation of an electrical network seems to suggest a thermodynamic interpretation. We have also seen that any FFG composed of the building blocks of the classical linear state space models can be translated into an equivalent electrical network. The electrical network "solves" the Kalman filtering (and smoothing) problem on a general graph. Carter's circuit-theory interpretation of Kalman filtering also fits nicely into this framework.

Some further relations between probabilistic models and electrical networks are discussed in [22]. For example, a probabilistic interpretation can be given to Tellegen's Theorem, to Green's reciprocity theorem, and to some electrical networks proposed in [16] for signal processing tasks.

Acknowledgments. Sanjoy Mitter of the Massachusetts Institute of Technology (MIT) directed our attention to the book by Dennis [6], which was a main source of inspiration for this work. Dani Lippuner of Siemens AG (formerly ETH Zürich), our coauthor of [21], pointed out to us the paper by Carter [3]. Bernhard C. Levy of the University of California in Davis made us aware of additional earlier work on Kalman filtering on graphs including [4] [5] [14]. Finally, we are indebted to G. David Forney, Jr., of the MIT, for detailed comments on an earlier version of this paper.

APPENDIX

Gaussian Distributions and Quadratic Forms. In this appendix, we briefly review two issues related to normal distributions: first, elimination of variables from an n-dimensional normal distribution by integration or maximization; second, the representation of the Dirac delta as a limit of normal distributions.

Let A^H denote Hermitian matrix transposition (i.e., transposition followed by elementwise complex conjugation). We will consider functions of the form

$$f(x) = e^{-q(x)} \tag{A.1}$$

with

$$q(x) \triangleq (x-m)^H W (x-m) + c \tag{A.2}$$
$$= x^H W x - 2\mathrm{Re}\big(x^H W m\big) + m^H W m + c, \tag{A.3}$$

where x is a real or complex vector, where W is a nonnegative definite $n \times n$ matrix, and where the constant $c \in \mathbb{R}$ amounts to a scale factor in (A.1) which can often be ignored. The case where all quantities in (A.2) are real-valued and $q(.)$ is a function $\mathbb{R}^n \to \mathbb{R}$ will be referred to as "the real case"; the case where $q(.)$ is a function $\mathbb{C}^n \to \mathbb{R}$ will be referred to as "the complex case". If W is positive definite, (A.1) may be viewed as a multi-dimensional normal probability density with mean vector m.

Integration and Maximization. (See for example [15]). Let

$$q(x,y) \triangleq \Big((x-m_X)^H,\, (y-m_Y)^H\Big) \begin{pmatrix} W_{1,1} & W_{1,2} \\ W_{2,1} & W_{2,2} \end{pmatrix} \begin{pmatrix} x-m_X \\ y-m_Y \end{pmatrix}, \tag{A.4}$$

where x and y are real or complex vectors and where the block matrix on the right-hand side of (A.4) is nonnegative definite with $W_{1,1}$ positive definite. Then

$$\int_x e^{-q(x,y)} \propto \max_x e^{-q(x,y)} \tag{A.5}$$
$$= e^{-\min_x q(x,y)}. \tag{A.6}$$

Dirac Delta as Limit of Gaussians. An n-dimensional Dirac delta can be obtained as a limit of normal distributions:

$$\delta(x) = \lim_{\beta\to\infty} \begin{cases} \gamma(\beta) e^{-\beta\|x\|^2}, & \text{if } \|x\|^2 < 1/\sqrt{\beta} \\ 0, & \text{else} \end{cases} \tag{A.7}$$

with $\gamma(\beta) = (\beta/\pi)^{n/2}$ in the real case and $\gamma(\beta) = (\beta/\pi)^n$ in the complex case. It is often convenient and permissible to simplify (A.7) to

$$\delta(x) = \lim_{\beta\to\infty} \gamma(\beta) e^{-\beta\|x\|^2}. \tag{A.8}$$

In this paper, as in [15], we have freely used this simplified version. However, a detailed discussion of its validity is outside the scope of this paper.

Note that, if (A.8) is valid, it is consistent with our use of "$\propto$" to write

$$\delta(x) \propto \lim_{\beta\to\infty} e^{-\beta\|x\|^2}. \tag{A.9}$$

In this paper, we have also used the following generalization of (A.7). We only state the sloppy version corresponding to (A.8). If V is a k-dimensional subspace of $\mathbb{R}^n$, we define

$$\delta(x \in V) \triangleq \lim_{\beta\to\infty} (\beta/\pi)^{(n-k)/2}\, e^{-\beta\|A_1^T x\|^2}, \tag{A.10}$$

where A_1 is an $n \times (n-k)$ matrix whose columns form an orthonormal basis of $V^\perp$, the orthogonal complement of V in $\mathbb{R}^n$. (This implies that $\|A_1^T x\|$ is the norm of the projection of x into $V^\perp$ and that $A_1^T A_1$ is an identity matrix.) Now let A_0 be an $n \times k$ matrix whose columns form an orthonormal basis of V and let $A = (A_0, A_1)$. (This implies $A_0^T A_1 = 0$ and $A^{-1} = A^T$.) We then can write

$$\delta(x \in V) = \lim_{\beta\to\infty} (\beta/\pi)^{(n-k)/2}\, e^{-\frac{1}{\beta}\|A_0^T x\|^2 - \beta\|A_1^T x\|^2} \tag{A.11}$$

$$= \lim_{\beta\to\infty} (\beta/\pi)^{(n-k)/2}\, e^{-x^T A D A^T x} \tag{A.12}$$

with

$$D \triangleq \operatorname{diag}\big(\underbrace{1/\beta, \ldots, 1/\beta}_{k \text{ times}}, \underbrace{\beta, \ldots, \beta}_{n-k \text{ times}}\big). \tag{A.13}$$

From (A.11) and (A.12), it is easy to see that

$$\delta(x \in V^\perp) = \lim_{\beta\to\infty} (\beta/\pi)^{k/2}\, e^{-x^T A D^{-1} A^T x} \tag{A.14}$$

$$= \lim_{\beta\to\infty} (\beta/\pi)^{k/2}\, e^{-x^T \left(A D A^T\right)^{-1} x}. \tag{A.15}$$

REFERENCES

[1] Special issue on "Codes on graphs and iterative decoding." *IEEE Trans. Inform. Theory,* vol. 47, no. 2, Feb. 2001.

[2] S. Boyd and L. Vandenberghe, *Convex Optimization.* Preprint of book, 2001.

[3] D. W. Carter, "A circuit theory of the Kalman filter," *Proc. 32nd Conf. on Decision and Control*, (San Antonio, TX, USA), pp. 1224–1226, Dec. 1993.

[4] A. P. Dempster, "Construction and local computation aspects of network belief functions," in *Influence Diagrams, Belief Nets, and Decision Analysis,* R. M. Oliver and J. Q. Smith, eds., Wiley 1990, pp. 121–141.

[5] A. P. Dempster, "Normal belief functions and the Kalman filter," Dept. Statistics Harvard Univ. Cambridge, May 1990.

[6] J. B. Dennis, *Mathematical Programming and Electrical Networks.* Jointly by MIT Press, John Wiley, and Chapman & Hall, 1959.

[7] G. D. Forney, Jr., "Codes on graphs: normal realizations," *IEEE Trans. Inform. Theory,* vol. 47, no. 2, pp. 520–548, 2001.

[8] R. G. Gallager, *Low-Density Parity-Check Codes.* Cambridge, MA: MIT Press, 1963.

[9] F. V. Jensen, *An Introduction to Bayesian Networks.* New York: Springer Verlag, 1996.

[10] M. I. Jordan and C. M. Bishop, *An Introduction to Graphical Models.* Draft of book, 2001.

[11] R. Kindermann and J. L. Snell, *Markov Random Fields and their Applications.* Providence, Rhode Island: American Mathematical Society, 1980.

[12] F. R. Kschischang, B. J. Frey, and H.-A. Loeliger, "Factor graphs and the sum-product algorithm," *IEEE Trans. Inform. Theory,* vol. 47, no. 2, pp. 498–519, 2001.

[13] S. L. Lauritzen and D. J. Spiegelhalter, "Local computations with probabilities on graphical structures and their application to expert systems (with discussion)," *J. Royal Stat. Soc., Series B,* vol. 50, pp. 157–224, 1988.

[14] B. C. Levy, A. Benveniste, R. Nikoukhah, "High-level primitives for recursive maximum-likelihood estimation," *IEEE Trans. Automatic Control,* vol. 41, pp. 1125–1145, Aug. 1996.

[15] H.-A. Loeliger, "Least squares and Kalman filtering on Forney graphs," in *Codes, Graphs, and Systems,* festschrift in honor of G. D. Forney, Jr., Kluwer, 2002.

[16] C. Mead, *Analog VLSI and Neural Systems.* Reading, MA: Addison-Wesley, 1989.

[17] J. Pearl, *Probabilistic Reasoning in Intelligent Systems,* 2nd ed. San Francisco: Morgan Kaufmann, 1988.

[18] R. T. Rockafellar, *Convex Analysis.* Princeton, N.J.: Princeton University Press, 1970.

[19] P. Rusmevichientong and B. Van Roy, "An analysis of belief propagation on the turbo decoding graph with Gaussian densities," *IEEE Trans. Inform. Theory,* vol. 47, pp. 745–765, Feb. 2001.

[20] R. M. Tanner, "A recursive approach to low complexity codes," *IEEE Trans. Inform. Theory,* vol. IT-27, pp. 533–547, Sept. 1981.

[21] P. O. Vontobel, D. Lippuner, and H.-A. Loeliger, "Kalman filtering, factor graphs, and electrical networks." *Proc. 15th Int. Symp. on Math. Theory of Networks and Systems,* South Bend, IN, USA, Aug. 12–16, 2002.

[22] P. O. Vontobel, *Kalman Filters, Factor Graphs, and Electrical Networks.* Internal report INT/200202, ISI-ITET, ETH Zurich, April 2002.

[23] Y. Weiss and W. T. Freeman, "On the optimality of the max-product belief propagation algorithm in arbitrary graphs," *IEEE Trans. Inform. Theory* vol. 47, no. 2, pp. 736–744, 2001.

[24] N. Wiberg, H.-A. Loeliger, and R. Kötter, "Codes and iterative decoding on general graphs," Europ. Trans. Telecomm., vol. 6, pp. 513–525, Sept/Oct. 1995.

[25] N. Wiberg, *Codes and Decoding on General Graphs.* Ph.D. thesis, Linköping University, Sweden, 1996.

[26] J. C. Willems, "Paradigms and puzzles in the theory of dynamical systems," *IEEE Trans. Automat. Control,* vol. 36, no. 3, pp. 259–294, 1991.